Article

The Comparative Toxic Impact Assessment of Carbon Nanotubes, Fullerene, Graphene, and Graphene Oxide in Marine Microalgae *Porphyridium purpureum*

Konstantin Pikula [1]*, Seyed Ali Johari [2], Ralph Santos-Oliveira [3,4] and Kirill Golokhvast [1,5]

[1] Polytechnical Institute, Far Eastern Federal University, 10 Ajax Bay, Russky Island, 690922 Vladivostok, Russia; pikula_ks@dvfu.ru (K.P.)
[2] Department of Fisheries, Faculty of Natural Resources, University of Kurdistan, Pasdaran St, Sanandaj 66177-15175, Iran; sajohari@gmail.com (S.A.J.)
[3] Laboratory of Nanoradiopharmaceuticals and Synthesis of Novel Radiopharmaceuticals, Nuclear Engineering Institute, Brazilian Nuclear Energy Commission, Rua Hélio de Almeida 75, 21941906 Rio de Janeiro, Brazil; roliveira@ien.gov.br (R.S.O.)
[4] Laboratory of Nanoradiopharmaceuticals and Radiopharmacy, Rio de Janeiro State University, R. São Francisco Xavier, 524, 23070200 Rio de Janeiro, Brazil
[5] Siberian Federal Scientific Centre of Agrobiotechnology, Centralnaya Str., Presidium, 633501 Krasnoobsk, Russia; golokhvast@sfsca.ru (K.G.)
* Correspondence: pikula_ks@dvfu.ru

Abstract: The growing production and application of carbon-based nanomaterials (CNMs) represent possible risks for aquatic systems. However, the variety of CNMs with different physical and chemical properties, and different morphology complicated the understanding of their potential toxicity. This paper aims to evaluate and compare the toxic impact of four most common CNMs, namely multiwalled carbon nanotubes (CNTs), fullerene (C60), graphene (Gr), and graphene oxide (GrO) in marine microalgae *Porphyridium purpureum*. The microalgae cells were exposed to the CNMs for 96 h and measured by flow cytometry. Based on the obtained results, we determined no observed effect level (NOEL), calculated EC10 and EC50 concentrations for growth rate inhibition, esterase activity, membrane potential, and reactive oxygen species (ROS) generation changes for each tested CNMs. According to the sensitivity (growth rate inhibition) of *P. purpureum*, the used CNMs can be listed in following order: CNTs > GrO > Gr > C60. The toxicity of CNTs was significantly higher than the toxic effect of the other used CNMs and only this sample caused increase of ROS generation in microalgae cells. This effect caused by trace metal residuals in CNTs and high affinity between particles and microalgae associated with the presence of exopolysaccharide coverage on *P. purpureum* cells.

Keywords: carbon nanomaterials; graphene family materials; bioassay; nanotoxicology; ecotoxicology; flow cytometry; growth rate inhibition

1. Introduction

Production and research on carbon-based nanomaterials (CNMs) undergo exponential growth over last decade [1-3]. In 2021 the global CNMs market was valued at $2.9 billion and projected to reach $31.6 billion by 2031 with a compound annual growth rate (CAGR) of 27.7% according to the report of Allied Market Research (https://www.alliedmarketresearch.com/carbon-nano-materials-market (accessed on 05 May 2023)). The main representatives of the family of CNMs are fullerene (C60 or C70), graphene (Gr), graphene oxide (GrO), carbon nanotubes (CNTs), carbon quantum dots, and other derivatives [4]. Freixa et al. (2018) stated in their analytical work that fullerenes are the most studied group of CNMs, followed by multiwalled carbon nanotubes (MWCNTs), single walled carbon nanotubes (SWCNTs), Gr, and black carbon [5]. The interest in CNMs based on its unique mechanical, electrical, thermal, optical, and chemical properties [6]. Consequently, this type of materials found application in various industrial processes and consumer products, such as drug

 doi:10.20944/preprints202305.0738.v1

carriers [2, 7], bio-sensors [8], compounds for bionanocomposites [9, 10], energy conversion and storage devices [11, 12], environmental purification [13, 14], recovery of valuable compounds such as rare earth elements and other metals [15, 16], etc.

The growing production and application of CNMs lead to rise in the risks of environmental contamination. CNMs could enter aquatic systems during life cycle of all the products containing CNMs including production, transportation, application, and disposal [17]. In this point of view, risk assessment of CNMs became a crucial problem for maintaining safe environment and minimize human health risks.

Among the main obstacles coupled with risk assessment of nanomaterials (NMs) in aquatic environment should be highlighted (1) dependence of toxic behavior on particle physical and chemical properties, and variety of sizes, shapes, surface area, functionalization, etc. [18-20], (2) fate and transformation of NMs in aquatic environment and in the contact with different organisms, which could alter initial toxicity of materials [21, 22], and (3) species specific toxicity [23, 24]. The following paragraphs briefly discuss these three points.

Particle size, functional groups, oxygen content, surface charges, hydrophobicity, and defect sites can be emphasized among the properties of CNMs defining its toxicity [24]. The generally accepted fact that shorter CNTs have higher toxicity [25], and SWCNTs are more toxic than MWCNTs [26, 27]. Moreover, well dispersed CNMs are more toxic than their aggregates [28]. The most likely explanation of this size-dependent toxicity is the larger specific surface area of smaller particles and higher interaction with membranes of organisms [29]. The dose-response relationship in the toxicity assessment of CNMs is generally considered as not linear, where test organisms may adapt to low concentrations and high concentrations cause strong negative response [30, 31]. The presence of functional groups is a controversial factor which reported as inhibitor or stimulator of the toxicity compared to pristine unmodified NMs [32-35]. Surface functionalization of CNMs often change their main toxic effect between mechanical damage and oxidative stress [32, 36].

The environmental transformation of CNMs could significantly change their toxicity. Colloidal behavior and biodegradation of carbon-based and graphene family nanomaterials in aquatic environment were reviewed in our previous work [21]. It was previously shown that the addition of natural organic matter (NOM) caused concentration-dependent disaggregation of fullerene C60 crystals and increased potential toxic effect [37]. It also has been reported that the stability of GrO increases in the presence of humic acid and decreases in the presence of polysaccharides [38]. In general, laboratory toxicity comparison of CNMs complicated with variations of the used exposure protocols, including type of NMs, exposure time, sample preparation methods, etc.

Based on the literature, the sensitivity to CNMs varied between aquatic species, where the most sensitive group of organisms were algae, followed by crustaceans, fish and bacteria [5]. Considering microalgae as one of the most sensitive organisms to CNMs, it should be mentioned that the toxic effect of CNMs to algal cells might be associated not only with direct exposure, but also with shading effect (light absorption and photosynthesis prevention) and nutrient depletion [39]. It also worth noting that the toxicity of CNMs varies between different microalgae species [40, 41]. Several studies reported overproduction of extracellular polymeric substances in algae exposed to high concentrations of CNMs as a defensive mechanism [42, 43].

This paper focused on the evaluation of toxic levels and toxic effects caused by the impact of four typical representatives of CNMs in marine microalgae. The chosen CNMs were multiwalled carbon nanotubes (CNTs), fullerene (C60), graphene powder (Gr), and graphene oxide (GrO). Microalgae was chosen as a sensitive and useful modes for NMs environmental risk assessment. In this work we used a red algae *Porphyridium purpureum* which is commonly used in ecotoxicology [44-46].

 doi:10.20944/preprints202305.0738.v1

2. Materials and Methods

2.1. Nanoparticles

In this work we used four types of CNMs (Table 1), namely multiwalled carbon nanotubes (CNTs), fullerene (C60), graphene powder (Gr), and graphene oxide (GrO). These types of NPs were chosen to compare the toxic effects and the impact between different CNMs in marine microalgae.

Table 1. Characteristics of the used carbon nanomaterials.

Sample	Size	Purity	Synthesis or manufacturer information
CNTs	Diameter: 6-13 nm; Length: 2.5-20 μm	> 98% (main trace metals: Al - 10000 ppm, Co – 2652 ppm)	Batch Number: MKCM1457; Sigma Aldrich, St. Louis, MO, USA
C60	Diameter: 0.8 nm	> 95.5% (oxide C60)	Batch Number: 120722; Modern Synthesis Technology (MST), Saint-Petersburg, Russia
Gr	Thickness: 3-10 nm; Diameter: 0.5-10 μm	> 99%	Type #1, CAS#: 1034343-98-0; Modern Synthesis Technology (MST), Saint-Petersburg, Russia
GrO	Diameter:10-100 μm	Carbon: 46%; Oxygen: 49%; Hydrogen: 2,5%; Sulfur: 2,5%	CAS#: 1034343-98-0; Modern Synthesis Technology (MST), Saint-Petersburg, Russia

2.2. Microalgae cultures and Exposure Protocol

The culture of a red alga *Porphyridium purpureum* (Bory de Saint-Vincent) Drew et Ross, 1965 (Rhodophyta) originally isolated from the Peter the Great Bay (Sea of Japan, Far Eastern Russia) were provided by the Resource Collection *Marine Biobank* of the National Scientific Center of Marine Biology, Far Eastern Branch of the Russian Academy of Sciences (NSCMB FEB RAS). The *P. purpureum* species (Figure S1) was chosen based on their abundance among microalgae in the Sea of Japan [47] and their suitability as test-organisms in ecotoxicology [48, 49]. The morphology and physiology of *P. purpureum* was carefully described before [50, 51].

Culturing of microalgae and toxicity test conditions were maintained following the guidance of OECD No.201 [63] with minor modifications as stated below. Microalgae were cultured with Guillard's f/2 medium [52]. Filtered (pore diameter of the filter was 0.22 μm) and sterilized seawater with salinity 33 ± 1‰, pH 8.0 ± 0.2 was used for the experiments. The cultivation was carried out at a temperature of 20 ± 2 °C with an illumination intensity of 300 μmol photons/m²s, and a light:dark cycle of 12:12 h.

Before the experiment microalgae cells were cultivated in 250 mL Erlenmeyer's flasks. Algal culture in the exponential growth phase was taken for bioassays. For the experiment, microalgae cells were transferred to 12-well plates where each well contained 2 mL of microalgae aliquots and 2 mL of the tested sample to facilitate. The initial cell density in each well was 5–6×10⁴ cells/mL. The wells of a control group had only microalgae aliquots with addition of 2 mL of f/2 medium. The other wells had different concentration of the prepared NP suspension.

The stock suspensions of the four used CNMs were prepared in filtered seawater to eliminate additional negative impact on microalgae associated with salinity reduction. The stock concentration for all the CNMs was 250 mg/mL. To prevent the agglomeration of NPs, the stock suspensions were sonicated with ultrasound homogenizer Bandelin Sonopuls GM 3100 (Bandelin Electronic GmbH & Co. KG, Germany) with the high-frequency power of 100W for 30 minutes. The sonication was performed on ice in 40 mL Sonopuls Rosette cell RZ-2 to prevent sample heating. The prepared stock

Preprints (www.preprints.org) | NOT PEER-REVIEWED | Posted: 10 May 2023 doi:10.20944/preprints202305.0738.v1

suspensions were used to obtain the final exposure concentrations of 1, 10, 25, 50, 75, 100, 125 mg/mL. Each concentration and control group were carried out in triplicate. The duration of microalgae exposure to the NPs was 96 h.

2.3. Flow Cytometry Measurement

The method of flow cytometry was used to evaluate the growth rate inhibition, size and biochemical changes in microalgae cells after the exposure to NPs. All the measurements were carried out with CytoFLEX flow cytometer (Beckman Coulter, Indianapolis, IN, USA) with the software package CytExpert v.2.5. The staining by specific fluorescent dyes was used to evaluate biochemical changes and distinguish live and dead microalgae cells. The used endpoints, biomarkers, and parameters of their registration are represented in Table 2. The excitation source and emission channels were selected according to the maximum emission of the used fluorescent dyes, provided by the manufacturer (Molecular Probes, Eugene, OR, USA). In all the cases, the excitation source was a blue laser (488 nm) of the CytoFLEX flow cytometer.

Table 2. Bioassay endpoints and registration parameters.

Endpoint	Fluorescent Dye or Registered Parameter	Duration of microalgae exposure before the measurement	Dye concentration / Duration of Staining *	Emission Channel / Band Width, nm
Growth inhibition	PI	96 h	20 μM/20 min	610/20
Size	Forward scatter intensity (size calibration kit F13838 by Molecular Probes, USA)	96 h	–	FSC
Esterase activity	FDA	24 h	100 μM/20 min	525/40
Membrane potential	$DiOC_6$	24 h	5 μM/20 min	525/40
ROS generation	H_2DCFDA	24 h	100 μM/40 min	525/40

ROS, Reactive oxygen species; PI, Propidium iodide; FDA, Fluorescein diacetate; DiOC6, 3,3′-dihexyloxacarbocyanine iodide; H_2DCFDA, 2',7'-dichlorodihydrofluorescein diacetate. * The optimization of the used concentrations and duration of staining were described in our previous work [49].

The determination and count of microalgae cells in the analyzed samples was carried out using the parameters of microalgae cell size, granularity, and fluorescence of chlorophyll *a* (emission channel 690 nm). The dead cells were excluded from the count by the presence of intensive fluorescence in 610 nm emission channel (PI positive cells).

For the measurement of esterase activity, membrane potential, and ROS generation, after 24 h of exposure, the sample from each well of 12-well plates was gently pipetted and 500 μL of liquid was transferred in 48-well plate and stained. The staining was made with PI and one of the other dyes. In general, all the measurements were performed three times separately, namely PI and FDA, PI and FDA, PI and H_2DCFDA. PI was used to exclude dead cells, FDA, $DiOC_6$, and H_2DCFDA were used to assess esterase activity, membrane potential, and ROS generation changes, respectively.

 doi:10.20944/preprints202305.0738.v1

The data of each well was collected at a flow rate of 100 µl/min until 2000 cells were registered. The mean fluorescence intensity (MFI) of the registered cells in the emission channel of 525 nm was used for comparison. For all the types of the used CNMs and for each couple of the dyes, negative and positive controls was measured directly before the measurement of the wells with exposed microalgae cells. Negative control group was prepared by 98 °C heat treatment of not exposed cells in dry block heater for 15 minutes. The wells with addition of only f/2 media were used as positive control. The obtained MFI data were normalized using positive control as 100% and negative control as 0%.

The growth rate inhibition was measured after 96 h of exposure. The sample from each well of 12-well plates was gently pipetted and 100 µL of liquid was transferred in 96-well plate and stained with only PI. The data of each well was collected at a flow rate of 100 µl/min for 30 sec. The obtained data was collected as number of cells per mL and then compared with the number of cells in control group. The changes in forward scatter intensity and the used size calibration kit allowed to compare the changes in cell size distribution after the exposure to CNMs.

Based on the results of growth rate inhibition, esterase activity, membrane potential, and ROS generation change assays, we calculated the effective concentrations of the CNMs, which caused 10% (EC10) and 50% (EC50) inhibition of listed endpoints. The calculation of EC10 and EC50 values were performed by nonlinear regression fit in GraphPad Prism 8.0.2 (GraphPad Software, San Diego, CA, USA).

2.4. Microscopy

Morphological changes of microalgae cells were observed and captured by optical microscope Axio Observer A1 (Carl Zeiss, Oberkochen, Germany).

2.5. Statistical Analysis

Statistical analyzes were performed by GraphPad Prism 8.0.2 (GraphPad Software, San Diego, CA, USA). The statistical significance was tested by one-way ANOVA. Normality residuals was checked by the Anderson-Darling test. A value of $p \leq 0.05$ was considered statistically significant.

3. Results

The no observable effect level (NOEL) and calculated effective concentrations of the four used CNMs which caused 10% (EC10) and 50% (EC50) inhibition of microalgal growth rate and corresponding changes in esterase activity, membrane potential, and ROS generation in microalgae cells are given in Table 3.

Preprints (www.preprints.org) | NOT PEER-REVIEWED | Posted: 10 May 2023 doi:10.20944/preprints202305.0738.v1

Table 3. The toxicity descriptors of CNMs exposure to *P. purpureum*, mg/L.

Descriptor	CNTs	C60	Gr	GrO
***Growth rate inhibition*, 96 h**				
NOEL. mg/L	<1	50	10	<1
EC10. mg/L	0.49 (0.4396–0.5494)	24.10 (10.24–67.41)	15.55 (9.479–22.97)	8.60 (7.727–9.553)
EC50. mg/L	2.08 (1.935–2.251)	>131.0	94.88 (83.68–108.5)	23.37 (21.84–24.98)
***Esterase activity inhibition*, 24 h**				
NOEL. mg/L	<1	<1	1	1
EC10. mg/L	1.01 (0.36–2.43)	57.12 (41.60–73.18)	14.48 (10.09–19.88)	8.44 (6.84–10.45)
EC50. mg/L	8.182 (5.014–12.44)	93.17 (83.68–102.6)	44.73 (38.82–50.92)	18.28 (16.67–20.02)
***Membrane potential change*, 24 h**				
NOEL. mg/L	25^{inh}	1^{sti}	$<1^{sti}$	$125^{n/a}$
EC10. mg/L	38.68 (26.24–50.00)^{inh}	$<1^{sti}$	$<1^{sti}$	n/a
EC50. mg/L	46.55 (39.39–49.55)^{inh}	17.40 (6.76–32.61)^{sti}	5.61 (1.16–12.69)^{sti}	n/a
***ROS generation change*, 24 h**				
NOEL. mg/L	10^{sti}	$125^{n/a}$	25^{inh}	25^{inh}
EC10. mg/L	10.82 (n/a)	n/a	27.90 (13.80–43.82)^{inh}	25.54 (13.64–37.77)^{inh}
EC50. mg/L	14.66 (n/a)	n/a	$>125^{inh}$	123.20 (106.30–153.00)^{inh}

inh, Inhibition effect; sti, stimulative effect; n/a, not assessed (the descriptor cannot be calculated).

Based on the obtained results, the tested CNMs can be listed depending on the level of toxic exposure in red microalgae *P. purpureum*. Therefore, the growth rate and esterase activity of microalgae reduce in the following order: CNTs > GrO > Gr > C60. Sample CNTs had the highest adverse effect on growth rate and esterase activity of the microalgae cells. Moreover, only this sample caused membrane depolarization ($DiOC_6$ fluorescence decrease) and significantly increased the level of ROS generation (increase in H_2DCFDA fluorescence) in microalgae cells. Samples C60 and Gr caused high membrane hyperpolarization in microalgae cells ($DiOC_6$ fluorescence increase). At the same time, GrO demonstrated no significant effect on cell membrane polarization even at the highest used concentration. It should be noted that sample C60, which had the lowest toxic impact in the microalgae, was the only used type of CNMs demonstrated no significant effect on ROS generation in the cells of *P. purpureum*.

The changes in esterase activity, membrane potential, and ROS generation depending on the concentration of the CNs are visualized in Figure 1. All the data of statistical significance calculations related to these parameters are listed in Table S1.

Preprints (www.preprints.org) | NOT PEER-REVIEWED | Posted: 10 May 2023 doi:10.20944/preprints202305.0738.v1

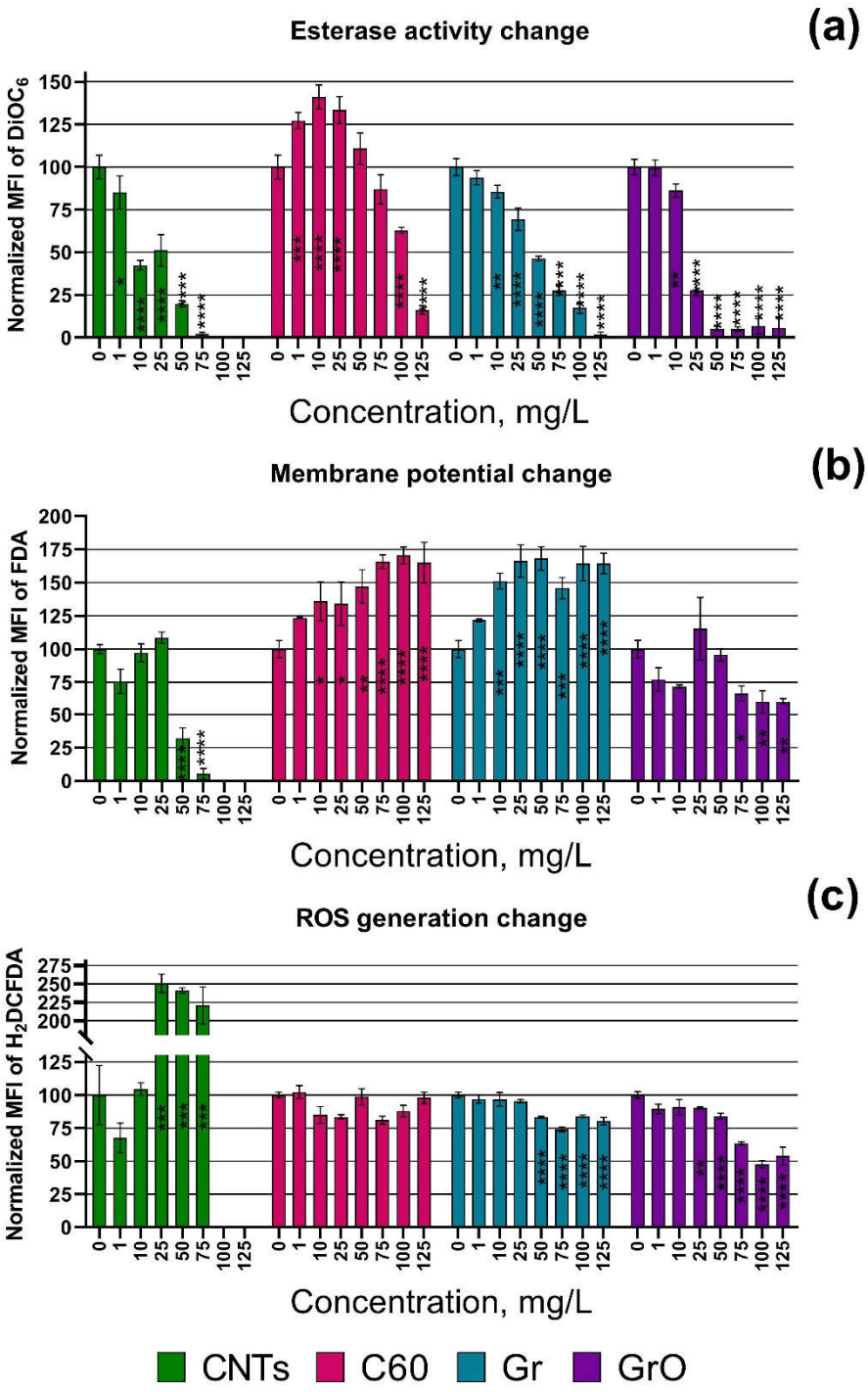

Figure 1. Biochemical changes in microalgae cells after 24 h of exposure to carbon nanomaterials: (**a**) esterase activity; (**b**) membrane potential; (**c**) Reactive oxygen species (ROS) generation. *, $p < 0.05$; **, $p < 0.005$; ***, $p < 0.0005$; ****, $p < 0.0001$. The used endpoints were calculated compared to control, where 0% is negative control (heat treated cells) and 100% is positive control (cells with no exposure to nanoparticles).

In addition to the data of Table 3, Figure 1a demonstrated that esterase activity of *P. purpureum* exposed to C60 increased at lower concentrations (1-25 mg/L), maintained normal level at middle concentrations (50-75 mg/L), and rapidly decreased at the higher concentrations (100-125 mg/L).

Preprints (www.preprints.org) | NOT PEER-REVIEWED | Posted: 10 May 2023 doi:10.20944/preprints202305.0738.v1

The changes in the size of *P. purpureum* cells are visualized in Figure 2. The data of statistical significance calculations related to the changes in cell size are listed in Table S2.

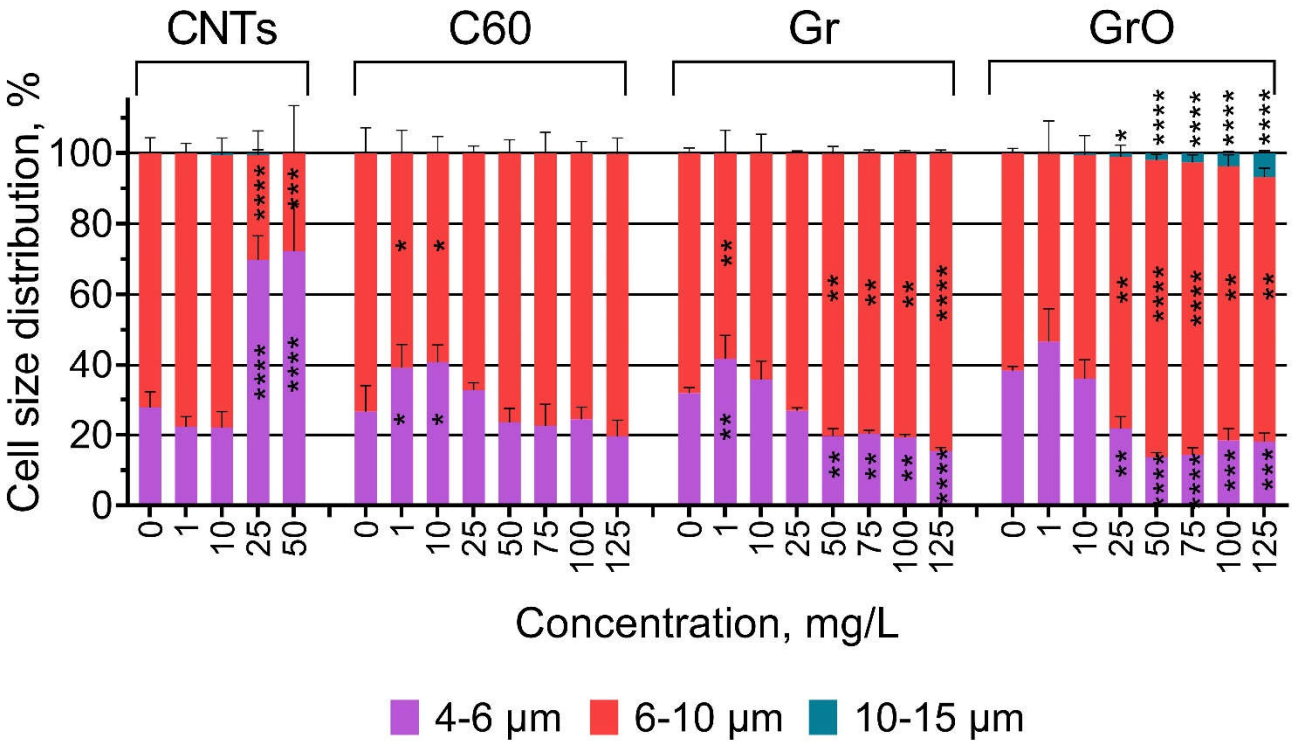

Figure 2. The changes in the size of *P. purpureum* cells after 96 h of exposure to carbon nanomaterials. *, $p < 0.05$; **, $p < 0.005$; ***, $p < 0.0005$; ****, $p < 0.0001$.

The highest toxic effect caused by the exposure of *P. purpureum* to CNTs (Table 3, Figure 1) correlates with decrease in the size of microalgae cells at concentrations of 25 and 50 mg/L. The low concentrations of samples C60 (1-10 mg/L) and Gr (1 mg/L) also caused moderate decrease in cell size. The higher concentrations of samples Gr (50-125 mg/L) and GrO (25-125 mg/L) caused noticeable increase in cell size. The most pronounced increase in cell size was observed after the exposure to GrO, and the concentrations of 25-125 mg/L evoked enlargement of the cells to the size more than 10 µm.

Preprints (www.preprints.org) | NOT PEER-REVIEWED | Posted: 10 May 2023 doi:10.20944/preprints202305.0738.v1

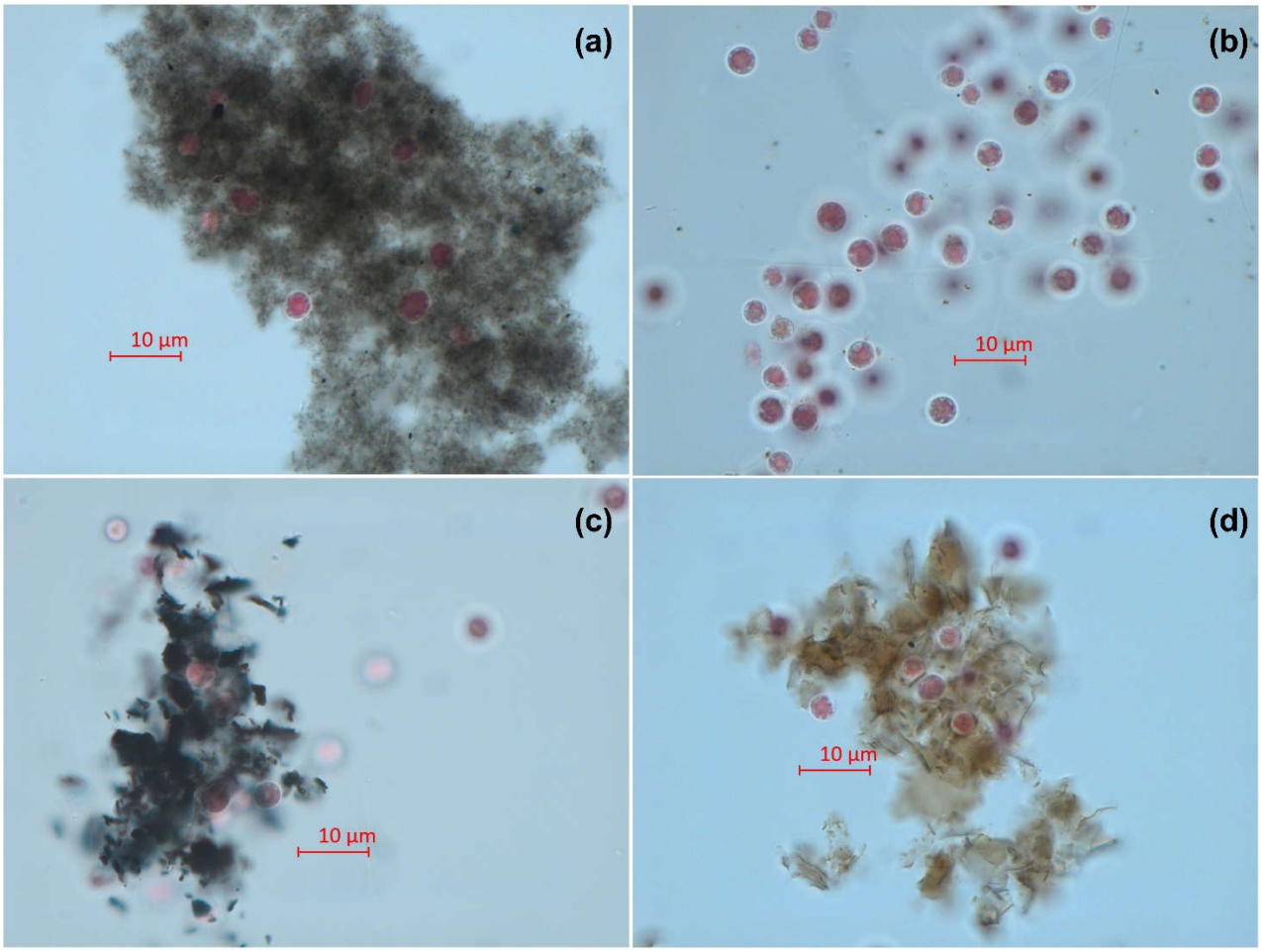

Figure 3. Microscopic pictures of *P. purpureum* after 96 h of exposure to carbon nanomaterials: (**a**) multiwalled carbon nanotubes (sample CNTs) at concentration of 50 mg/L; (**b**) fullerene (sample C60) at concentration of 125 mg/L; (**c**) graphene powder (sample Gr) at concentration of 125 mg/L; (**d**) graphene oxide (sample GrO) at concentration of 125 mg/L. Magnification 1000 ×.

The microscopic observation demonstrated that the cells of *P. purpureum* can agglomerate with the big clusters of CNMs. This effect occurred in the cases of CNTs (Figure 3a), Gr (Figure 3c), and GrO (Figure 3d). C60 did not forms clusters and demonstrated lower affinity to *P. purpureum* cells, but small particles of C60 was absorbed to the surface of microalgae cells (Figure 3b).

4. Discussion

Although CNMs are assumed as a substances with relatively low toxicity [17, 53], they has a great variety of allotropic forms which could demonstrate different toxic properties in different species and conditions [54, 55]. The present study was designed to determine the differences in the effect of multiwalled carbon nanotubes, fullerene, graphene powder, and graphene oxide in marine microalgae *P. purpureum*.

In our previous work, a red algae *P. purpureum* was more sensitive to the exposure of CNTs compare to thee the other marine microalgae species because of a highly hydrophobic surface of *P. purpureum* cells covered with exopolysaccharide coverage [40]. It is known that the surface properties of CNMs is one of the determinant factors of their toxicity [56, 57]. The properties of graphene family nanomaterials and related biological interactions were carefully described in the work of Sanchez et al. 2011 [58]. Fu and Zhang (2018) in their work explained the relationship between adhesion and hydrophobicity of NPs [59]. Consequently, hydrophobic NPs would have higher affinity to

 doi:10.20944/preprints202305.0738.v1

hydrophobic regions of the cell membrane and result in higher potential of accumulation and penetration across the cells [59, 60].

In this work, all the used CNMs did not have any functionalization or surface coatings and initially had hydrophobic properties. Among the tested samples, the highest hydrophobicity demonstrated sample CNTs, which rapidly agglomerated in seawater after the sonication at high concentrations, and probably had higher adhesion with *P. purpureum* cells. This assumption correlate with the fact that CNTs were found to cause significantly higher toxic effect (Table 3) in the microalgae compare to the other used nanomaterials. Moreover, fullerene C60 revealed the lowest toxicity toward microalgae cells (Table 3) and was the only used CNM did not formed clusters in seawater even at the highest used concentration (125 mg/L) and demonstrated lower adhesion with the cells (Figure 3b).

It is known that graphene family NMs could directly penetrate into the cell membrane of algae through cell pores [61-63]. It was reported that GrO enters into the cells of *Chlorella vulgaris* and damage organelles, enhanced the generation of ROS, and disrupted antioxidant enzymes [64]. On the contrary, our study revealed decrease of ROS generation in *P. purpureum* under the exposure to GrO (Figure 1c).

As demonstrated in Figure 3, the agglomerated flakes of CNTs, Gr, and GrO were sedimented and covered microalgae cells. In this case, it is important to notice the role of shading effect in the toxicity of CNMs. In photosynthetic microorganisms like microalgae or cyanobacteria CNMs prevent the illumination of the cells due to light absorption CNMs [41, 65]. This effect could limit photosynthetic activity and growth rate of microalgae cells, and cause metabolic disruption [41]. This effect might be the reason of observed cell size change in *P. purpureum* exposed to high concentrations of CNTs, Gr, and GrO (Figure 2).

It is known that unlike graphene family nanomaterials, CNTs are grown catalytically and often contain residual metal catalysts [58]. The presence of trace metal residuals is another factor caused higher toxicity of CNTs in microalgae [66]. The used sample of CNTs contain residuals of Al and Co (Table 1). Although Co is one of the essential metals for cell function, it may become toxic at high concentrations [67, 68]. It was reported that Al induced oxidative stress, ultrastructural changes, changes in lipid metabolism, degradation of cellular organelles, and suppression of antioxidant enzymatic activity in microalgae [69, 70]. These facts explain ROS generation increase in *P. purpureum* cells after the exposure to CNTs (Figure 1c). Intensive ROS formation causes destruction in proteins, lipids, and carbohydrates, and lead to oxidative stress in microalgae [68].

Previous work demonstrated that oxidized multiwalled CNTs and GrO caused esterase enzyme inhibition but no oxidative stress in cyanobacteria *Microcystis aeruginosa*, and EC50 level 7.38 and 11.1 mg/L for CNTs and GrO, respectively [71]. These results are in agreement with the results of current study (Table 3) in fact that CNTs had higher cytotoxicity in microalgae than GrO. Several works shown that Gr was more toxic than CNTs in microalgae *Scenedesmus obliquus* and *Chlorella pyrenoidosa* [39, 72], The other study with *Scenedesmus obliquus* stated a higher toxicity of Gr compared to GrO [61]. The results of these studies did not agree with our work as the sensitivity of *P. purpureum* to the tested CNMs had the following order: CNTs > GrO > Gr > C60. Current observations reveal the importance of multispecies toxicity assessment and the role of surface properties both of microalgae cells and CNMs.

Considering the surface properties of CNMs in aquatic environment, it should be highlighted that NPs inevitably undergo not only physical transformation (agglomeration, sedimentation, etc.) but also obtain surface modification as a result of interaction with NOM, absorption of proteins and "biomolecular corona" formation [21, 73]. This issue attracts attention of scientific community [74, 75] and required further study in order to extend the understanding of fate and toxicity of CNMs. The "biomolecular corona" formation was not assessed in current work, nevertheless, this phenomenon should be taken into account in further study.

 doi:10.20944/preprints202305.0738.v1

5. Conclusions

This study revealed different level and toxic effects of four CNMs, namely multiwalled carbon nanotubes, fullerene, graphene powder, and graphene oxide in microalgae *P. purpureum.* In general, the growth rate and esterase activity of microalgae reduce in the following order: CNTs > GrO > Gr > C60. All the used CNMs except fullerene C60 strongly agglomerated in seawater forming relatively big clusters and agglomerated with microalgae cells facilitating mechanical damage and metabolic disorder associated with shading effect. CNTs was the only sample caused increase in ROS generation by microalgae cells, which is caused by trace metal residuals in CNTs. The finding of this study highlighted the importance of surface properties of CNMs and microalgae cells in toxicity bioassays. Following studies should consider the interaction of CNMs with NOM and the problem of "biomolecular corona" formation.

Supplementary Materials: Figure S1: Microscopic picture of *P. purpureum* from control group; Table S1: The statistical significance calculation of esterase activity, membrane potential, and ROS generation in *P. purpureum* cells after 24 h of exposure; Table S2: The statistical significance calculation of the changes in *P. purpureum* cells after 96 h of exposure.

Author Contributions: Conceptualization, K.P.; methodology, K.P. and S.A.J.; validation, R.S.A.; investigation, K.P.; resources, S.A.J. and R.S.A.; writing—original draft preparation, K.P.; writing—review and editing, K.G.; visualization, K.P.; project administration, K.P.; funding acquisition, K.P. All authors have read and agreed to the published version of the manuscript.

Funding: The work was supported by the Russian Science Foundation (RSF), project number 21-74-00023.

Institutional Review Board Statement: Not applicable.

Informed Consent Statement: Not applicable.

Data Availability Statement: Not applicable.

Conflicts of Interest: The authors declare no conflict of interest.

References

1. Jordan, C.C., I. Kaiser, and V.C. Moore, *2013 nanotechnology patent literature review: Graphitic carbon-based nanotechnology and energy applications are on the rise.* Nanotech. L. & Bus., 2014. **11**: p. 111.
2. Debnath, S.K. and R. Srivastava, *Drug delivery with carbon-based nanomaterials as versatile nanocarriers: progress and prospects.* Frontiers in Nanotechnology, 2021. **3**: p. 644564.
3. Zhang, J.-N., *Carbon-Based Nanomaterials for Energy Conversion and Storage: Applications in Electrochemical Catalysis*. Vol. 325. 2022: Springer Nature.
4. Mishra, R. and J. Militky, *Nanotechnology in textiles: theory and application*. 2018: Woodhead Publishing.
5. Freixa, A., et al., *Ecotoxicological effects of carbon based nanomaterials in aquatic organisms.* Science of the Total Environment, 2018. **619**: p. 328-337.
6. Zhou, X., et al., *Production, structural design, functional control, and broad applications of carbon nanofiber-based nanomaterials: A comprehensive review.* Chemical Engineering Journal, 2020. **402**: p. 126189.
7. Maiti, D., et al., *Carbon-based nanomaterials for biomedical applications: a recent study.* Frontiers in pharmacology, 2019. **9**: p. 1401.
8. Eivazzadeh-Keihan, R., et al., *Applications of carbon-based conductive nanomaterials in biosensors.* Chemical Engineering Journal, 2022: p. 136183.
9. Makvandi, P., et al., *Biofabricated nanostructures and their composites in regenerative medicine.* ACS Applied Nano Materials, 2020. **3**(7): p. 6210-6238.
10. Liu, H., et al., *Carbon-based nanomaterials for bone and cartilage regeneration: a review.* ACS Biomaterials Science & Engineering, 2021. **7**(10): p. 4718-4735.

11. Yogeswari, B., et al., *Role of carbon-based nanomaterials in enhancing the performance of energy storage devices: Design small and store big.* Journal of Nanomaterials, 2022. **2022**.
12. Zhu, C.-y., et al., *Design and synthesis of carbon-based nanomaterials for electrochemical energy storage.* New Carbon Materials, 2022. **37**(1): p. 59-92.
13. Liu, D., et al., *Recent advances in MOF-derived carbon-based nanomaterials for environmental applications in adsorption and catalytic degradation.* Chemical Engineering Journal, 2022. **427**: p. 131503.
14. Smith, S.C. and D.F. Rodrigues, *Carbon-based nanomaterials for removal of chemical and biological contaminants from water: A review of mechanisms and applications.* Carbon, 2015. **91**: p. 122-143.
15. Cardoso, C.E., et al., *Recovery of rare earth elements by carbon-based nanomaterials—a review.* Nanomaterials, 2019. **9**(6): p. 814.
16. Iftekhar, S., et al., *Porous materials for the recovery of rare earth elements, platinum group metals, and other valuable metals: a review.* Environmental Chemistry Letters, 2022. **20**(6): p. 3697-3746.
17. De Marchi, L., et al., *An overview of graphene materials: properties, applications and toxicity on aquatic environments.* Science of the Total Environment, 2018. **631**: p. 1440-1456.
18. Nam, S.-H. and Y.-J. An, *Size-and shape-dependent toxicity of silver nanomaterials in green alga Chlorococcum infusionum.* Ecotoxicology and Environmental Safety, 2019. **168**: p. 388-393.
19. Saleh, T.A., *Nanomaterials: Classification, properties, and environmental toxicities.* Environmental Technology & Innovation, 2020. **20**: p. 101067.
20. Czarnecka, J., et al., *Cytotoxic or not? Disclosing the toxic nature of carbonaceous nanomaterials through nano–bio interactions.* Materials, 2020. **13**(9): p. 2060.
21. Pikula, K., S.A. Johari, and K. Golokhvast, *Colloidal Behavior and Biodegradation of Engineered Carbon-Based Nanomaterials in Aquatic Environment.* Nanomaterials, 2022. **12**(23): p. 4149.
22. Williams, R.J., et al., *Models for assessing engineered nanomaterial fate and behaviour in the aquatic environment.* Current opinion in environmental sustainability, 2019. **36**: p. 105-115.
23. Vasyukova, I., et al., *Toxic Effect of metal-based nanomaterials on representatives of marine ecosystems: A review.* Nanobiotechnology Reports, 2021. **16**: p. 138-154.
24. Malhotra, N., et al., *Toxicity studies on graphene-based nanomaterials in aquatic organisms: Current understanding.* Molecules, 2020. **25**(16): p. 3618.
25. Cheng, J. and S.H. Cheng, *Influence of carbon nanotube length on toxicity to zebrafish embryos.* International journal of nanomedicine, 2012: p. 3731-3739.
26. Lawrence, J., et al., *Effects of fullerene (C60), multi-wall carbon nanotubes (MWCNT), single wall carbon nanotubes (SWCNT) and hydroxyl and carboxyl modified single wall carbon nanotubes on riverine microbial communities.* Environmental Science and Pollution Research, 2016. **23**: p. 10090-10102.
27. Kavosi, A., et al., *The toxicity and therapeutic effects of single-and multi-wall carbon nanotubes on mice breast cancer.* Scientific reports, 2018. **8**(1): p. 1-12.
28. Kowk, K.W.H., et al., *Chronic toxicity of double-walled carbon nanotubes to three marine organisms: influence of different dispersion methods.* Nanomedicine, 2010. **5**(6): p. 951-961.
29. Kobayashi, N., H. Izumi, and Y. Morimoto, *Review of toxicity studies of carbon nanotubes.* Journal of occupational health, 2017. **59**(5): p. 394-407.
30. Guerard, M., et al., *Assessment of mechanisms driving non-linear dose–response relationships in genotoxicity testing.* Mutation Research/Reviews in Mutation Research, 2015. **763**: p. 181-201.
31. Bell, I.R., J.A. Ives, and B.J. Wayne, *Nonlinear effects of nanoparticles: biological variability from hormetic doses, small particle sizes, and dynamic adaptive interactions.* Dose-Response, 2014. **12**(2): p. dose-response. 13-025. Bell.

32. Zhou, L., et al., *Multi-walled carbon nanotubes: a cytotoxicity study in relation to functionalization, dose and dispersion.* Toxicology in vitro, 2017. **42**: p. 292-298.
33. Sasidharan, A., et al., *Differential nano-bio interactions and toxicity effects of pristine versus functionalized graphene.* Nanoscale, 2011. **3**(6): p. 2461-2464.
34. Li, R., et al., *Surface charge and cellular processing of covalently functionalized multiwall carbon nanotubes determine pulmonary toxicity.* ACS nano, 2013. **7**(3): p. 2352-2368.
35. Figarol, A., et al., *Biological response to purification and acid functionalization of carbon nanotubes.* Journal of nanoparticle research, 2014. **16**: p. 1-12.
36. Alshehri, R., et al., *Carbon nanotubes in biomedical applications: factors, mechanisms, and remedies of toxicity: miniperspective.* Journal of medicinal chemistry, 2016. **59**(18): p. 8149-8167.
37. Xie, B., et al., *Impact of natural organic matter on the physicochemical properties of aqueous C60 nanoparticles.* Environmental science & technology, 2008. **42**(8): p. 2853-2859.
38. Lanphere, J.D., et al., *Stability and transport of graphene oxide nanoparticles in groundwater and surface water.* Environmental engineering science, 2014. **31**(7): p. 350-359.
39. Zhao, J., et al., *Mechanistic understanding toward the toxicity of graphene-family materials to freshwater algae.* Water Research, 2017. **111**: p. 18-27.
40. Pikula, K., et al., *Comparison of the Level and Mechanisms of Toxicity of Carbon Nanotubes, Carbon Nanofibers, and Silicon Nanotubes in Bioassay with Four Marine Microalgae.* Nanomaterials, 2020. **10**(3): p. 485.
41. Schwab, F., et al., *Are Carbon Nanotube Effects on Green Algae Caused by Shading and Agglomeration?* Environmental Science & Technology, 2011. **45**(14): p. 6136-6144.
42. Verneuil, L., et al., *Multi-walled carbon nanotubes, natural organic matter, and the benthic diatom Nitzschia palea:"A sticky story".* Nanotoxicology, 2015. **9**(2): p. 219-229.
43. Garacci, M., et al., *Few Layer Graphene sticking by biofilm of freshwater diatom Nitzschia palea as a mitigation to its ecotoxicity.* Carbon, 2017. **113**: p. 139-150.
44. Pikula, K., et al., *The Impact of Metal-Based Nanoparticles Produced by Different Types of Underwater Welding on Marine Microalgae.* Toxics, 2023. **11**(2): p. 105.
45. Grant, T.M., et al., *Towards eco-friendly marine antifouling biocides–Nature inspired tetrasubstituted 2, 5-diketopiperazines.* Science of The Total Environment, 2022. **812**: p. 152487.
46. Bauddh, K. and J. Korstad, *Phycoremediation: use of algae to sequester heavy metals.* Hydrobiology, 2022. **1**(3): p. 288-303.
47. Orlova, T.Y., I. Stonik, and O. Shevchenko, *Flora of planktonic microalgae of Amursky Bay, Sea of Japan.* Russian Journal of Marine Biology, 2009. **35**(1): p. 60-78.
48. Markina, Z.V., et al., *Porphyridium purpureum microalga physiological and ultrastructural changes under copper intoxication.* Toxicology reports, 2021. **8**: p. 988-993.
49. Pikula, K.S., et al., *Toxicity assessment of particulate matter emitted from different types of vehicles on marine microalgae.* Environmental Research, 2019. **179**: p. 108785.
50. Aizdaicher, N., I. Stonik, and A. Boroda, *The development of Porphyridium purpureum (Bory de Saint-Vincent) Drew et Ross, 1965 (Rhodophyta) from Amursky Bay, Sea of Japan, in a laboratory culture.* Russian Journal of Marine Biology, 2014. **40**(4): p. 279-285.
51. Schornstein, K.L. and J. Scott, *ULTRASTRUCTURE OF CELL-DIVISION IN THE UNICELLULAR RED ALGA PORPHYRIDIUM-PURPUREUM.* Canadian Journal of Botany-Revue Canadienne De Botanique, 1982. **60**(1): p. 85-97.
52. Guillard, R.R. and J.H. Ryther, *Studies of marine planktonic diatoms. I. Cyclotella nana Hustedt, and Detonula confervacea (cleve) Gran.* Canadian journal of microbiology, 1962. **8**: p. 229-39.

53. Thines, R., et al., *Application potential of carbon nanomaterials in water and wastewater treatment: a review.* Journal of the Taiwan Institute of Chemical Engineers, 2017. **72**: p. 116-133.
54. Hinzmann, M., et al., *Nanoparticles containing allotropes of carbon have genotoxic effects on glioblastomamultiforme cells.* International Journal of Nanomedicine, 2014. **9**: p. 2409.
55. Kharisov, B.I. and O.V. Kharissova, *Carbon Allotropes in the Environment and Their Toxicity.* Carbon Allotropes: Metal-Complex Chemistry, Properties and Applications, 2019: p. 639-652.
56. Nel, A.E., et al., *Understanding biophysicochemical interactions at the nano–bio interface.* Nature materials, 2009. **8**(7): p. 543-557.
57. Kumar, P., et al., *Antibacterial properties of graphene-based nanomaterials.* Nanomaterials, 2019. **9**(5): p. 737.
58. Sanchez, V.C., et al., *Biological interactions of graphene-family nanomaterials: an interdisciplinary review.* Chemical research in toxicology, 2012. **25**(1): p. 15-34.
59. Fu, W. and W. Zhang, *Measurement of the surface hydrophobicity of engineered nanoparticles using an atomic force microscope.* Physical Chemistry Chemical Physics, 2018. **20**(37): p. 24434-24443.
60. Pogodin, S., N.K. Slater, and V.A. Baulin, *Surface patterning of carbon nanotubes can enhance their penetration through a phospholipid bilayer.* ACS nano, 2011. **5**(2): p. 1141-1146.
61. Zhang, Y., et al., *Humic acid alleviates the ecotoxicity of graphene-family materials on the freshwater microalgae Scenedesmus obliquus.* Chemosphere, 2018. **197**: p. 749-758.
62. Hazeem, L.J., et al., *Toxicity effect of graphene oxide on growth and photosynthetic pigment of the marine alga Picochlorum sp. during different growth stages.* Environmental Science and Pollution Research, 2017. **24**: p. 4144-4152.
63. Long, Z.F., et al., *Systematic and Quantitative Investigation of the Mechanism of Carbon Nanotubes' Toxicity toward Algae.* Environmental Science & Technology, 2012. **46**(15): p. 8458-8466.
64. Hu, X., et al., *Interactions between graphene oxide and plant cells: Regulation of cell morphology, uptake, organelle damage, oxidative effects and metabolic disorders.* Carbon, 2014. **80**: p. 665-676.
65. Nguyen, M.K., J.-Y. Moon, and Y.-C. Lee, *Microalgal ecotoxicity of nanoparticles: An updated review.* Ecotoxicology and Environmental Safety, 2020. **201**: p. 110781.
66. Ge, C., et al., *The contributions of metal impurities and tube structure to the toxicity of carbon nanotube materials.* NPG Asia Materials, 2012. **4**(12): p. e32-e32.
67. Leonardo, T., et al., *Determination of elemental distribution in green micro-algae using synchrotron radiation nano X-ray fluorescence (SR-nXRF) and electron microscopy techniques–subcellular localization and quantitative imaging of silver and cobalt uptake by Coccomyxa actinabiotis.* Metallomics, 2014. **6**(2): p. 316-329.
68. Liang, S.X.T., et al., *Toxicity of metals and metallic nanoparticles on nutritional properties of microalgae.* Water, Air, & Soil Pollution, 2020. **231**: p. 1-14.
69. Ameri, M., et al., *Aluminium triggers oxidative stress and antioxidant response in the microalgae Scenedesmus sp.* Journal of plant physiology, 2020. **246**: p. 153114.
70. Trenfield, M.A., et al., *Aluminium, gallium, and molybdenum toxicity to the tropical marine microalga Isochrysis galbana.* Environmental toxicology and chemistry, 2015. **34**(8): p. 1833-1840.
71. Cruces, E., et al., *Similar toxicity mechanisms between graphene oxide and oxidized multi-walled carbon nanotubes in Microcystis aeruginosa.* Chemosphere, 2021. **265**: p. 129137.
72. Das, S., et al., *Comparative ecotoxicity of graphene, functionalized multiwalled CNT and their mixture in freshwater microalgae, Scenedesmus obliquus: Analysing the role of oxidative stress.* 2023.
73. Neagu, M., et al., *Protein bio-corona: critical issue in immune nanotoxicology.* Archives of toxicology, 2017. **91**: p. 1031-1048.

 doi:10.20944/preprints202305.0738.v1

74. García-Hevia, L., et al., *The unpredictable carbon nanotube biocorona and a functionalization method to prevent protein biofouling.* Journal of Nanobiotechnology, 2021. **19**(1): p. 1-13.
75. Braccia, C., et al., *The lipid composition of few layers graphene and graphene oxide biomolecular corona.* Carbon, 2021. **185**: p. 591-598.